Malaysian Journal of Chemistry, 2025, Vol. 27(2), 54-63

Chemical Characterization of Monomeric and Polymeric Silicate Dropout from Ethylene Glycol-Based Coolant under the Effects of Metasilicate Dosage and Temperature

Siong Fong Sim[1]*, Nur Syazrin Habsah binti Ismail[1], Leong Seng Wong[1], Ivan Teo Yen Khai[1], William Liang[2] and Clarence Chin[2]
[1]Faculty of Resource Science & Technology, Universiti Malaysia Sarawak, 94300 Kota Samarahan, Sarawak, Malaysia
[2]Hexa BRT Sdn. Bhd., Lot 922, Block 7 MTLD, Jalan Demak Laut 3, Demak Laut Industrial Park, 93050, Kuching, Sarawak, Malaysia
*Corresponding author (e-mail: sfsim@unimas.my)

Ethylene glycol (EG)-based coolants help dissipate excess heat generated by engines, with sodium metasilicate often added as a corrosion inhibitor. However, adding metasilicate to EG coolant can lead to the formation of silicate gel, which compromises the coolant's efficiency. This gel-like precipitate is known as silicate dropout. This paper reports on the characteristics of silicate dropout from EG coolant under varying dosages of metasilicate and temperatures. The silicate precipitates were extracted and analyzed using Fourier Transform Infrared (FTIR) Spectroscopy to identify molecular bonding and structural changes. Field Emission Scanning Electron Microscopy (FE-SEM) was employed to examine the surface morphology and microstructural features of the precipitates. The study found that silicate dropout occurred when the metasilicate concentration reached 3% at room temperature. As the metasilicate dosage increased, the solubility of the silicate precipitates decreased due to saturation. This was evidenced by a reduction in absorption at 780, 850, and 1001 cm^{-1}. Elevated temperatures further facilitated silicate precipitation as a result of the exothermic nature of the reaction. The IR spectra demonstrated shifts in Si-O-Si bands to higher (954-845 cm^{-1} to 1001 – 854 cm^{-1}) and lower frequencies (811-699 cm^{-1} to 783 – 583 cm^{-1}), indicating the formation of a silicate network and the disruption of monomeric structures. The SEM images showed monomeric silicates at lower concentrations and temperatures, while polymeric structures dominated at higher temperatures and dosages. Energy Dispersive X-ray (EDX) analysis confirmed an increase in Si content within the precipitates at higher temperatures.

Keywords: Sodium metasilicate; silicate dropout; solubility; functional groups; morphology

Received: September 2024; Accepted: November 2024

Coolant is a crucial component in automotive systems. Typically, coolant consists of water as the base fluid, combined with an antifreeze solution, i.e., ethylene glycol or propylene glycol in a ratio of 50:50. This antifreeze solution lowers the freezing point and raises the boiling point of the coolant. The main function of coolant is to dissipate the excessive heat generated by the engine, which is essential for maintaining optimal operating temperatures and preventing overheating [1]. However, water-based coolants are prone to corrosion. To address this, corrosion inhibitors such as phosphonates, borates, and silicates are added in small quantities to protect against corrosion.

Sodium silicate (Na_2SiO_3) is an inorganic compound commonly added to coolants to form protective silicate layers that inhibit corrosion. In water, sodium silicate dissociates, forming sodium ions (Na^+) and silicate anions (SiO_3^{2-}, SiO_4^{4-}); which remain stable due to the repulsion between negatively charged silicate ions. When silicate ions come in contact with metal surfaces, they adsorbed onto the metal surfaces via electrostatic interactions. In the presence of water, these silicate ions undergo hydrolysis, forming bonds with metal oxides or hydroxides on the surface. The silicate ions then polymerize, creating an interconnected network that offers a protective film. A minimum concentration of 0.2 g/L has been established as necessary for the formation of stable surface film to effectively prevent corrosion [2, 3, 4]. Although sodium metasilicate is widely used in coolants, silicate-containing coolants experience a significant issue of silicate gel formation. When neutralized silicates polymerize excessively under altered pH, temperature and concentration, they form a three-dimensional network that expands and traps water molecules and other ions within the matrix, leading to the formation of a gel-like substance. This phenomenon is known as silicate dropout. The formation of silicate gel decreases the efficiency of the cooling system and shortens the coolant's shelf life. Additionally, the gel can cause blockages in the passages of the cabin heater and radiator, leading to overheating or inadequate heating, particularly in cold weather [5]. This issue impacts the cooling system's performance, presenting both physical and chemical challenges [6]. The gelation is influenced by factors such as pH, temperature, and silicate concentration [5]. While using a silicate stabilizer can mitigate this problem, it has the drawback of causing rapid depletion of silicate inhibitors [7].

Despite ongoing developments in new coolant formulations, the issue of silicate gelation persists. Research on silicate gelation in coolants is limited; therefore, this study aims to characterize the monomeric and polymeric silicate dropout from ethylene glycol-based coolant under varying silicate dosage and temperature. The findings of this study would provide insights into the behavior of silicate dropout, which can support the advancement of coolant development.

MATERIALS AND METHODS

1. Preparation of Coolant

A 50 mL coolant solution was prepared by mixing ethylene glycol (EG) and deionized water in a 50:50 ratio. Five different concentrations of sodium metasilicate (Na_2SiO_3) at 1.5%, 2%, 2.5%, 3%, and 5% (wt/vol) were mixed with the coolant. The mixture was shaken until all salts dissolved. The bottle was sealed and kept at room temperature for 3 days. The EG-based coolant with varying concentrations of Na_2SiO_3 was prepared and kept in an oven at 75°C, 90°C, and 110°C for 3 days. The initial pH before and after 3 days were measured using a pH meter. After 3 days, the formation of silicate dropout was observed and recorded. Solutions with silicate dropout were centrifuged for 30 minutes at 4000 rpm to separate out the dropout. The gel was dried in an oven at 105°C for 7 hours and subjected to analysis using Fourier Transform Infrared Spectroscopy (FTIR) and Field Emission Scanning Electron Microscopy (FE-SEM).

2. Fourier Transform Infrared (FTIR) Spectroscopy

The dried silica dropout was characterized using an Attenuated Total Reflectance Fourier Transform Infrared (ATR-FTIR) spectrometer with a diamond crystal (Thermo Fisher Scientific, Nicolet iS10). The spectra were acquired at a resolution of 8 cm^{-1} with 32 scans, and the scan range was set from 4000 to 400 cm^{-1}. Each sample of silica dropout was analyzed in triplicates. A background spectrum was collected and subtracted from the sample spectra. Following each measurement, the diamond plate was cleaned twice with absolute ethanol and subsequently dried. A total of 45 spectra were collected for 15 samples. The spectra, saved as .csv files, were extracted and analyzed in MATLAB R2013a.

The spectra were imported into Matlab for analysis using the automated peak detection and matching algorithm developed by [8]. Briefly, the spectra were baseline corrected and peaks in all spectra were identified using the first derivative approach. The peaks determined were then matched across all spectra to produce a peak table, with rows representing samples and columns denoting wavenumbers.

3. Field Emission Scanning Electron Microscopy (FE-SEM)

The dried silica dropout was examined using a scanning electron microscope (FE-SEM) (JEOL JSM-6390LA). A small amount of sample (approx. 5 mg) was directly applied to a conductive double-sided carbon tape on a plate. After ensuring that the sample adhered to the tape, a small blower was used to remove any excess sample. The surface morphology of the dropout was observed. Energy-Dispersive X-Ray (EDX) analysis was conducted to determine the elemental compositions.

The experimental design and workflow are illustrated in Figure 1.

RESULTS AND DISCUSSION

Table 1 summarizes the observations of silicate dropout at varying concentrations under the effect of temperature. No precipitate was observed in coolant containing 1.5%, 2%, 2.5%, and 3% metasilicate at room temperature after 3 days, except the samples of 5% metasilicate. In all other samples at increased temperatures. The silicate dropout at room temperature and 75°C was soft, spongy, and gelatinous. In contrast, the dropout at 90°C and 110°C was crystal-like powder. Higher concentrations of metasilicate, specifically 3% and 5%, resulted in higher amounts of dropout, especially at higher temperatures (110°C). As the gelling temperature increases, the time taken for silica to drop out decreases [9]. At higher temperatures, the kinetic energy of the particles increases, leading to higher speeds and a higher probability of collisions and aggregation [10]. Toghnovi et al. described the forms of silicate gel obtained according to pH and silicate concentrations. Silicate solution of < 3 mol/L at pH 9-11 is clear. When the silicate concentration increases to <4.5 mol/L, the gel formed is transparent and reversible. With an increase in silicate concentration to < 6.5 mol/L, the gel turns white and is soluble. The continuous increase in silicate eventually facilitates the formation of white, irreversible gel [11].

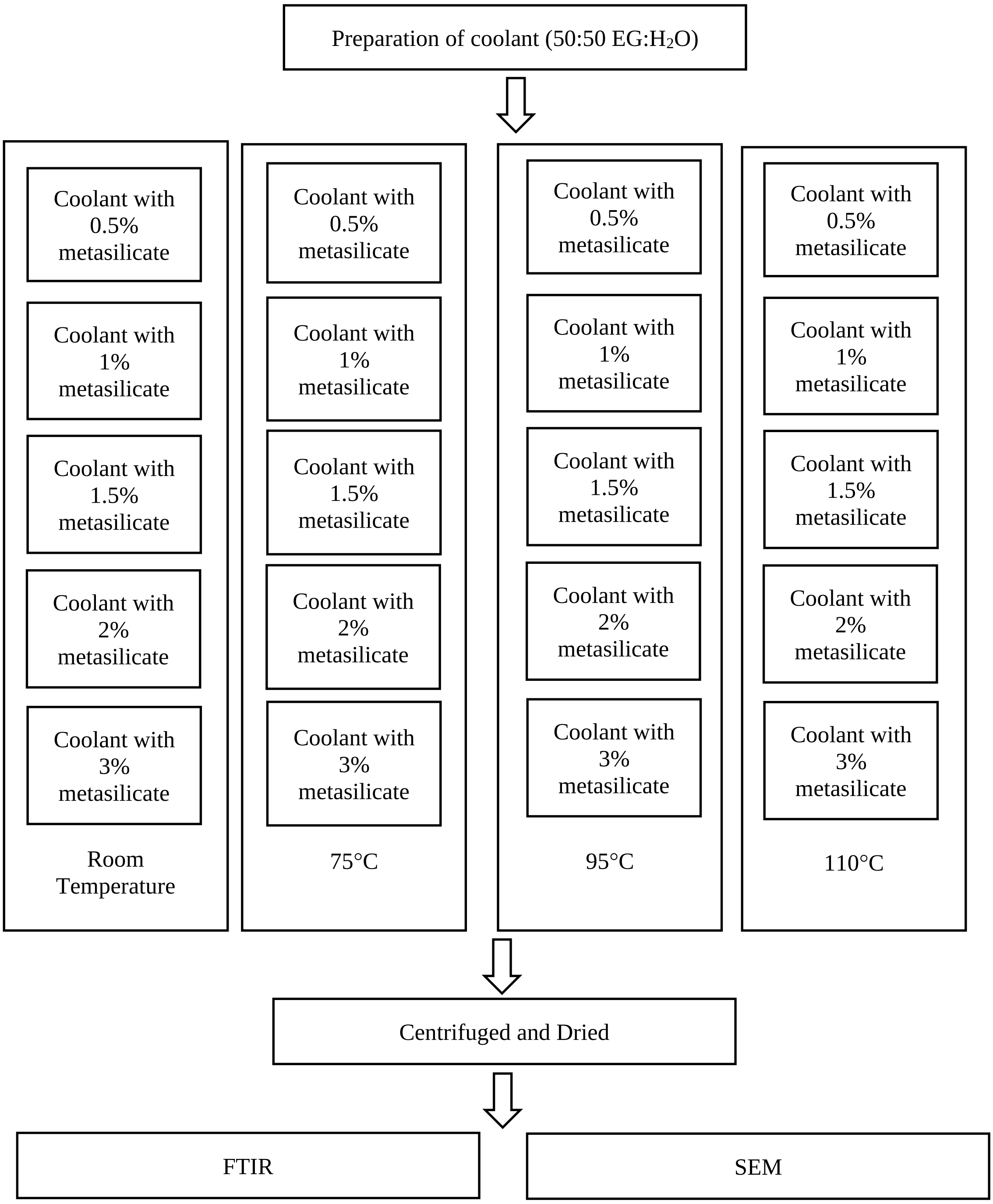

Figure 1. Experimental design and workflow.

Table 1. Observations of silicate dropout under varying metasilicate concentrations and temperatures.

Metasilicate concentration, %	**Room temperature**	**75°C**	**90°C**	**110°C**
1.5	Not observed	Not observed	Dropout	Dropout
2.0	Not observed	Dropout	Dropout	Dropout
2.5	Not observed	Dropout	Dropout	Dropout
3.0	Not observed	Dropout	Dropout	Dropout
5.0	Dropout	Dropout	Dropout	Dropout

Table 2. pH of coolant with varying metasilicate concentrations at different temperatures.

Metasilicate, %	Temperature, °C	Initial	After 3 days
1.50%	Room temperature	11.93	12.10
	75	11.60	11.81
	90	12.03	11.96
	110	12.02	11.97
2%	Room temperature	12.04	12.15
	75	12.04	11.93
	90	12.12	12.12
	110	12.1	12.02
2.50%	Room temperature	12.14	12.22
	75	12.1	11.98
	90	12.16	12.22
	110	12.16	12.08
3%	Room temperature	12.18	12.26
	75	12.14	12.01
	90	12.18	12.22
	110	12.21	12.15
5%	Room temperature	12.22	12.22
	75	12.22	12.22
	90	12.28	12.28
	110	12.28	12.21

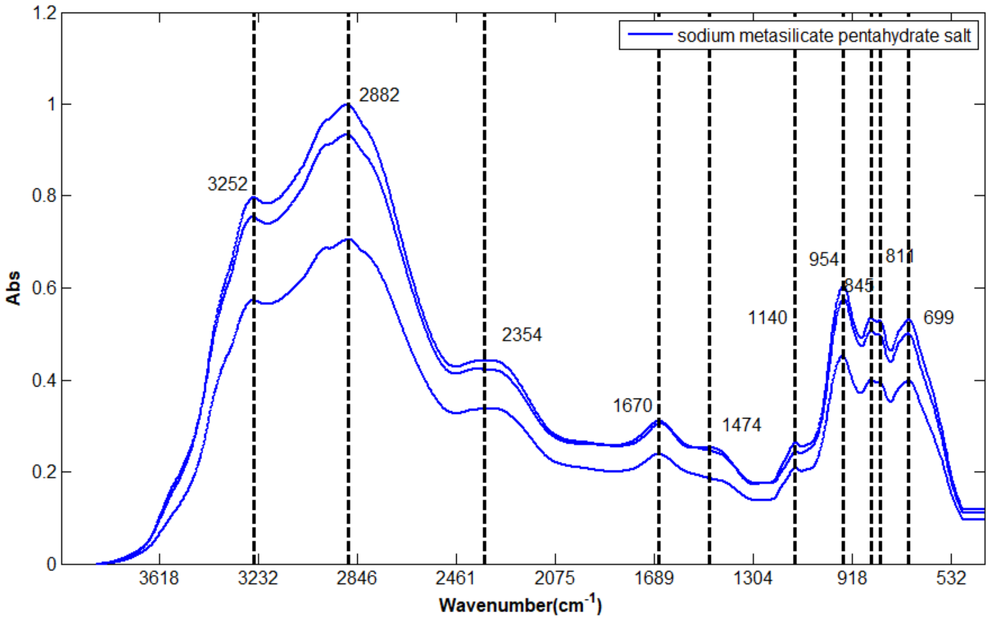

Figure 2. FTIR spectra of sodium metasilicate pentahydrate salt in triplicates.

The initial and final pH of the coolant with varying metasilicate concentrations at different temperatures are summarized in Table 2. Generally, there was a slight increase in pH after 3 days for coolants at room temperature across varying dosages, except at 5%. At higher temperatures, the pH fluctuated marginally. These pH changes are associated with the dynamic equilibrium between hydrolysis and polymerization of monomeric, oligomeric, and polymeric SiO_2 under different conditions, which affect the solubility and stability of SiO_2 [12]. Metasilicate salts exhibit better solubility at room temperature in low doses; however, as temperature and dosage increase, their solubility decreases.

Figure 2 presents the infrared (IR) spectra of sodium metasilicate pentahydrate salt. The spectra exhibited characteristics of water with broad absorption bands in the regions of 3300-2800 cm^{-1} and 1670-1640 cm^{-1}. The silanol groups (Si-OH) and siloxane bonds (Si-O-Si) were represented by the absorption bands at 946 cm^{-1} and 850-800 cm^{-1}, respectively [13-17]. The absorption band at 3450-2800 cm^{-1} was further assigned to the stretching vibration of silanol (Si-OH) groups and the O-H vibration of bound water [18].

The IR spectra of silicate dropout from varying EG solution under varying temperatures are shown in Figure 3. Precipitates at lower concentrations of 2% (75°C) and 2.5% (75°C and 90°C) exhibited significant baseline shifting. This is because of the low amount of dropout attained at these concentration levels, hence multiple times of centrifugation were performed to collect sufficient samples for analysis. This repeated processing could have induced physical or chemical changes in the samples. Additionally, the homogeneity of the dropout may have been compromised, contributing to the observed baseline shifts. For this reason, these samples of higher baseline were excluded from the analysis.

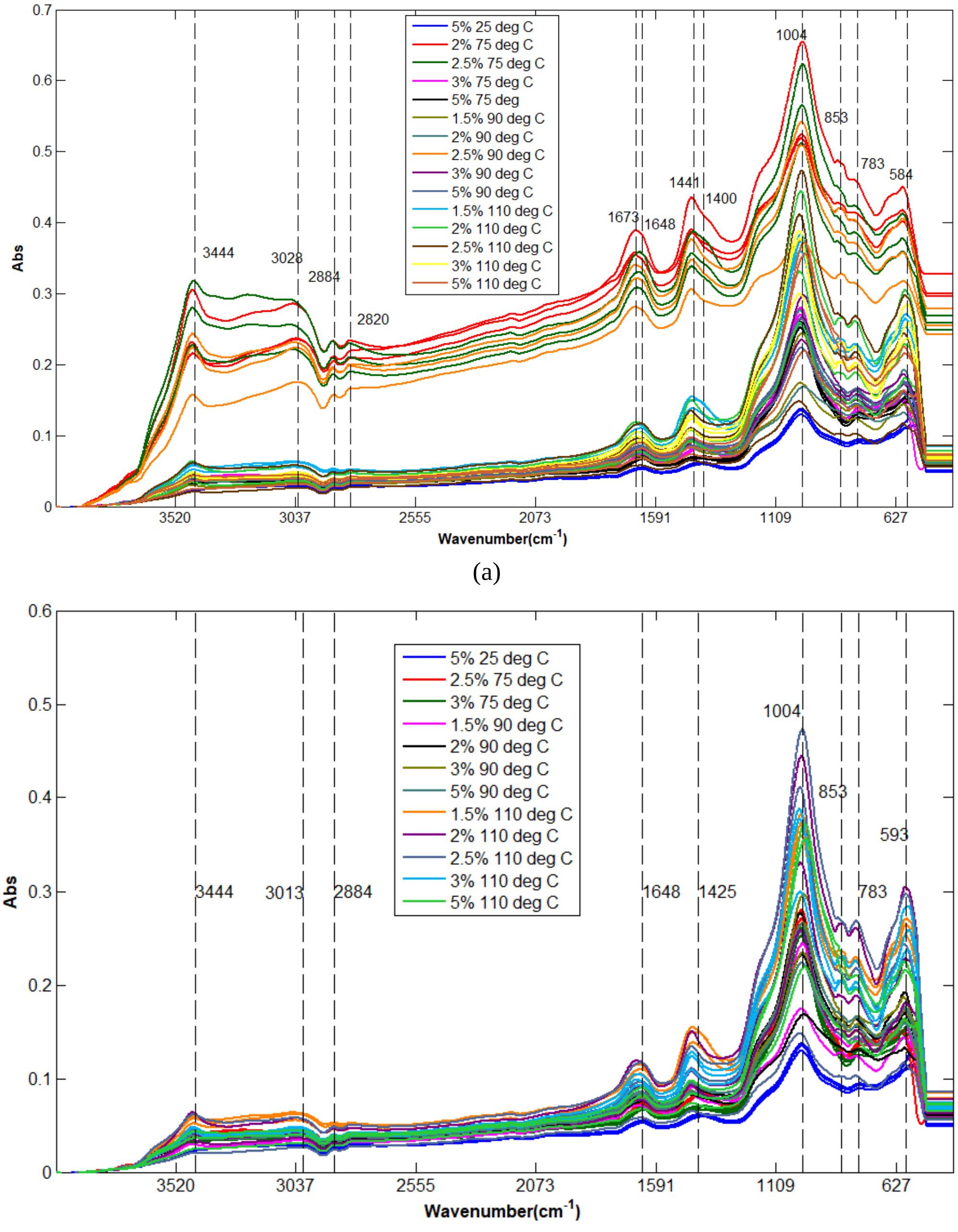

(a)

(b)

Figure 3. IR spectra of silicate dropout at varying concentrations and temperatures: (a) all spectra and (b) all spectra excluding spectra for 2% (75°C) and 2.5% (75°C and 90°C).

The spectra demonstrated several major absorption bands at 600, 780, 850, 1001, 1420, 1645, 2880, and 3400 cm^{-1}. The absorptions at 3010 and 1645 cm^{-1} were attributed to the stretching and bending vibrations of water, respectively. The absorption at 850, 780, and 1100 cm^{-1} were assigned to symmetric and asymmetric stretching of Si-O-Si linkages. Comparing with the spectra of sodium metasilicate salt (Figure 2), it was observed that the absorption bands at 954 and 845 cm^{-1} shifted to higher frequencies at 1004 and 853 cm^{-1} in the dropout. The observed shifts to higher frequencies in the absorption bands suggests a structural alteration in the Si-O bonds, leading to a more rigid structure in the precipitate. This increased rigidity likely results from a higher degree of polymerization, which involves the formation of more cross-linked or condensed silicate structures. In a more extensive silicate network, the Si-O-Si bond vibrations experience an increase in bond strength due to this polymerization. As a result, these stronger bonds absorb at higher frequencies, which is reflected in the observed shifts in the IR spectra. In 1990, Taylor demonstrated the IR band development of Na_2-Si_nO_{2n+1} at different degrees of polymerization [19]. As *n* decreased from 5 to 3 and then to 2, the absorption band at 1046 cm^{-1} shifted to 982 and 941 cm^{-1}, respectively.

In contrast, for the absorptions at 811 and 699 cm^{-1}, the bands appeared to develop at lower frequencies in the precipitate (783 and 583 cm^{-1}). These bands are mainly attributed to the bending vibrations of silicate structures. Taylor observed shifts in silicate bands from 781 cm^{-1} to 768 and 760 cm^{-1} as the network polymerization decreased from 5 to 3 to 2 [17]. A shift to a lower frequency suggests a disruption in the Si-O-Si network, leading to the formation of more non-bridging oxygens, such as Si-OH. The opposing shifts at ~950-900 and 800-700 cm^{-1} suggest that the precipitate underwent structural changes involving both polymerization and depolymerization, leading to heterogeneous structures. Some regions may become more tightly bonded, while others are less interconnected. Almeida et al. reported both red shifts and blue shifts in silica gel, attributing these changes to variations in the Si-O-Si bond angles and bond lengths at the surface of the gel pores [20].

Figure 4 presents the IR spectra of precipitates at various concentrations in EG solution under different temperatures. The characteristic vibration associated with polymeric SiO_2 at 1001 cm^{-1} was consistently observed across all temperature and dosage levels, with its peak area increasing as both temperature and dosage increased. A similar trend was noted for the lower-frequency vibrations at 850 and 780 cm^{-1}, which are indicative of monomeric SiO_2, suggesting the co-presence of both monomeric and polymeric SiO_2 in the samples. Notably, these lower-frequency absorptions were absent in precipitates formed at lower temperatures. Specifically, at a concentration of 3% and 75°C, the absorptions at 850 and 780 cm^{-1} were absent, signifying the prominent presence of polymeric SiO_2 and the greater solubility of monomeric SiO_2 at lower temperatures.

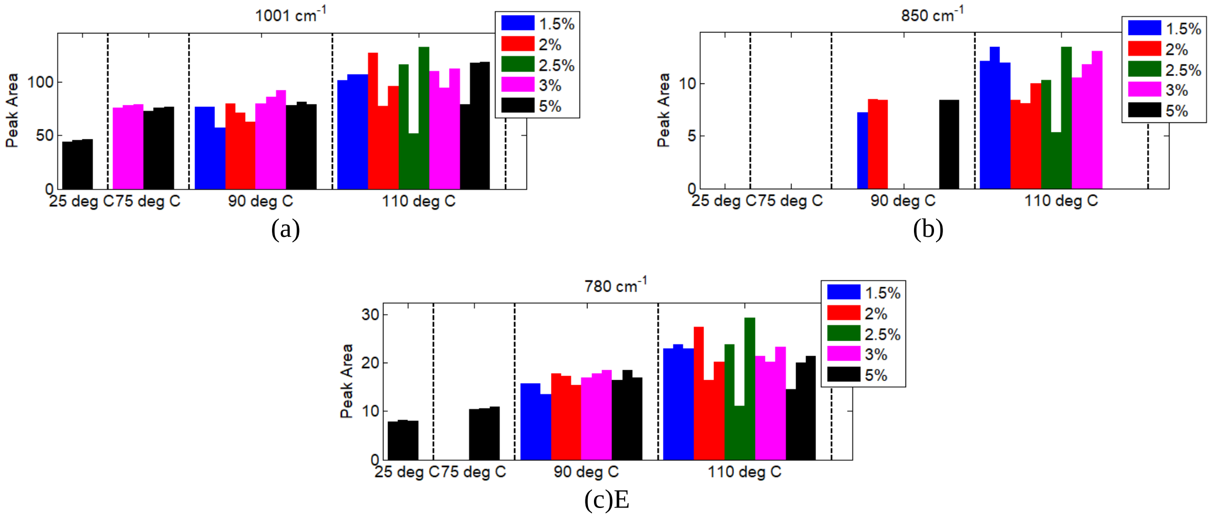

(a)

(b)

(c)E

Figure 4. Abundance of Si-O-Si bands at (a) 1001 cm^{-1}, (b) 850 cm^{-1}, and (c) 780 cm^{-1} for silicate precipitates obtained under different temperatures.

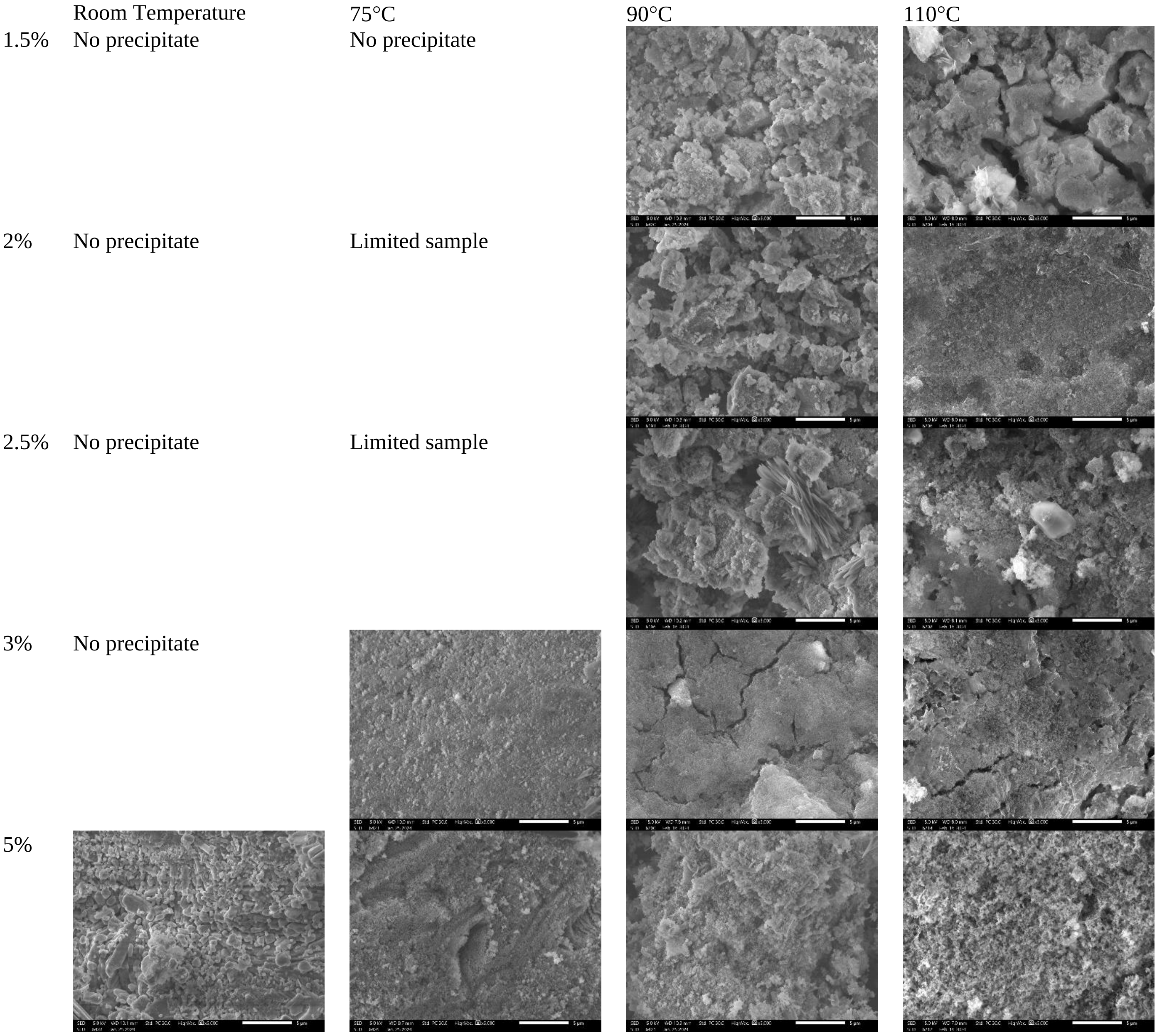

Figure 5. Scanning electron micrographs of dried silica gel obtained under different temperatures and metasilicate dosage at 5,000× magnification.

With increasing temperatures, the peaks of silicates at 780, 850, and 1001 cm^{-1} demonstrated an increase in abundance, as shown in Figure 3. This increase in peak abundance at higher temperatures is because the solubility of silicates in EG tends to decrease, promoting precipitation. The dissolution of sodium silicates in alcohol is an exothermic process that involves the cleavage of intermolecular bonds within the solid microstructure [21]. According to Le Chatelier's Principle, in an exothermic reaction, increasing the temperature will shift the equilibrium to favor the undissolved state of metasilicates, thus reducing their solubility and enhancing precipitation. Furthermore, increasing the dosage of metasilicate can cause the solution to reach saturation, which also reduces solubility and promotes precipitation.

Figure 5 shows the scanning electron micrographs of dried silica gel obtained under different temperatures and metasilicate dosage at 5,000× magnification. For 2% and 2.5% concentrations at 75°C, the silicate dropout was insufficient for SEM analysis. At lower concentrations, the silicate precipitates displayed well-defined crystal faces and were more distinctly separated. As the concentration increased, the particles became more densely packed and exhibited greater aggregation. Under the effect of temperature, particles at lower temperatures showed better definition, while higher temperatures led to morphology with less distinct crystal structures. Monomeric SiO_2 generally forms well-defined and more homogeneous particles, whereas polymeric SiO_2 tends to create larger aggregates with varied sizes and shapes [22]. The SEM images of precipitates at higher dosages and temperatures revealed a more pronounced polymeric SiO_2 morphology with increased aggregation.

Figure 6 shows the EDX spectra of silicate dropout at low (1.5%) and high (5%) concentration at 90°C. The spectra revealed the presence of Si, Na, C, and O in the precipitates, with their compositions varying according to dosage and temperature. The elemental compositions from the EDX analysis of the silicate precipitates are summarized in Table 3. Notably, the abundance of Si in the precipitates increases with temperature, while the solubility of Na decreases. The Si ratio ranges from 0.26 to 0.66. Deviations from the stoichiometric Si ratio of 1:2 may be attributed to the presence of water and Si-OH groups on the sample surface, which can affect the oxygen content. This study investigated the characteristics of silicate gel under varying dosages and temperatures. In another study, the formation of silica gel under different pH conditions was examined. It was reported that gelation involves three stages - induction, gelation, and over-curing - where gelation time increases with rising pH, and the system is characterized by non-stoichiometrically balanced reactions [23]. Silica gel formed in acidic pH was reported to have relatively smaller particles (pores < 550 nm) compared to that formed in alkaline condition (pores ~5 µm) [24]. The structure and distribution of silicate mainly depend on solute concentration, silica to alkali ratio, pH as well as temperature [25].

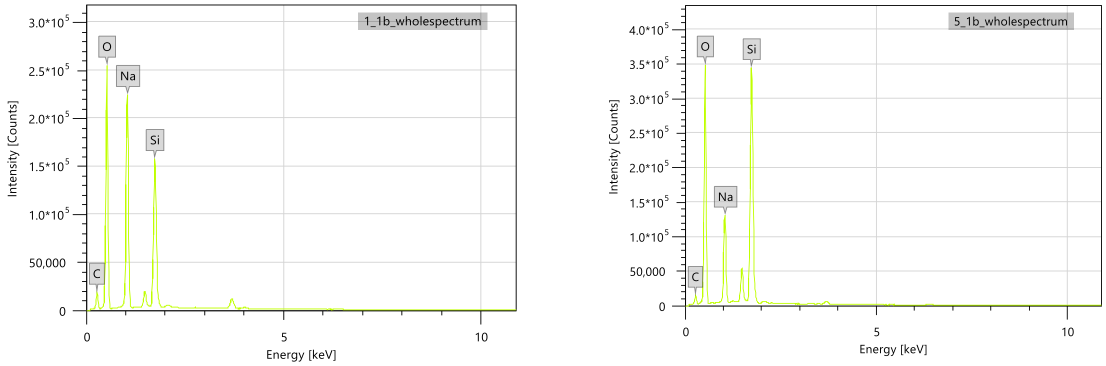

(a) 1.5% at 90 °C

(b) 5% at 90 °C

Figure 6. EDX spectra of silicate dropout at (a) 1.5% and (b) 5% at 90°C.

Table 3. Compositions of Si, Na, and O in silicate precipitates according to dosage and temperature.

Concentration, %	Temperature, °C	% Si	% Na	% O	Si/O
1.5	Room Temperature	-	-	-	-
	75	-	-	-	-
	90	13.08	25.46	50.06	0.26
	110	27.42	9.98	51.38	0.53
2	Room Temperature	-	-	-	-
	75	-	-	-	-
	90	22.70	4.77	47.94	0.47
	110	34.77	5.96	55.19	0.63
2.5	Room Temperature	-	-	-	-
	75	-	-	-	-
	90	28.55	8.75	53.57	0.53
	110	30.13	14.94	48.77	0.61
3	Room Temperature	-	-	-	-
	75	22.49	19.6	53.04	0.42
	90	29.28	9.34	56.48	0.51
	110	34.43	7.33	51.82	0.66
5	Room Temperature	6.06	34.65	48.25	0.12
	75	31.07	10.62	54.01	0.57
	90	22.16	13.1	56.53	0.39
	110	33.34	9.18	50.35	0.66

CONCLUSION

The study investigated the chemical characteristics of silicate precipitates from EG coolant containing different concentrations of metasilicate, subjected to different temperatures. It was found that silicate precipitation occurred when the metasilicate concentration in EG exceeded 3% at room temperature. As temperature increased from room temperature to 100°C, the solubility of silicates decreased due to the exothermic nature of the reaction; this was demonstrated based on the increased abundance of FTIR absorption bands for Si-O-Si at 1001, 870, and 780 cm^{-1}. At higher dosages and temperatures, the silicate precipitates exhibited a more polymeric structure due to saturation effects. This was evidenced by a more pronounced absorption band of polymeric silicate at 1001 cm^{-1}, corroborated by the presence of larger aggregates in SEM images. The precipitates obtained from coolant containing varying metasilicate concentrations, stored at different temperatures, primarily consisted of Na (4.77-34.65%), Si (6.06-34.43%, and O (47.94-56.53%). At elevated temperatures, Na solubility increased, as indicated by the decreasing %Na in the precipitates (e.g., 34.65% at room temperature to 9.18% at 110°C), while Si tended to precipitate, with an increasing %Si (6.06% at room temperature to 33.34% at 110°C).

ACKNOWLEDGEMENT

The authors thank Hexa BRT Sdn. Bhd. for funding this project (GL/F07/HEXA/2021). The authors also thank Universiti Malaysia Sarawak for supporting this work.

CONFLICT OF INTEREST

The authors declare that there is no conflict of interest.

REFERENCES

1. Habeeb, H. A., Mohan, A. E., Norani, N. A. M., Abdullah, M. A., Harun, M. H. (2020) Analysis of engine radiator performance at different coolant concentrations and radiator materials. *International Journal of Recent Technology and Engineering*, **8 (6)**, 2664–2669.

2. De Ketelaere, E., Moed, D., Vanoppen, M., Verliefde, A. R. D., Verbeken, K., Depover, T. (2023) Sodium silicate corrosion inhibitor behaviour for carbon steel in a dynamic saltwater environment. *Journal of Corrosion Science*, **217**, 2–10.

3. Yang, J., Li, Z., Shi, J., Yan, Z. (2023) Study on the corrosion inhibition performance of sodium silicate and polyaspartic acid for 35CrMo steel. *International Journal of Electrochemical Science*, **18 (4)**, 2–8.

4. Wiggle, R. R., Hospadaruk, V., Tibaudo, F. M. (1981) Corrosion of cast aluminum alloys under heat-transfer conditions. *SAE Technical Paper*, **810038**, 1–15.

5. Hercamp, R. D., Hudgens, R. D. (1985) Silicate gelation in heavy-duty diesel engine cooling systems. *SAE Technical Paper*, **852327**, 1–20.

6. Le Maout Alvarez, C., Minne, Anaïs., Le Saux, W., Cantrel, L., Simonnot, M. O. (2023) Characterization of precipitates susceptible to clogging of sump filters after a loss-of-coolant-accident in powers. *Chemical Engineering Research and Design*, **189**, 734–744.

7. Van de Ven, P., Maes, J. P. (1994) The effect of silicate content in engine coolants on the corrosion protection of aluminum heat-rejecting surfaces. *SAE Technical Paper Series*.

8. Sim, S. F., Ting, W. (2012) An automated approach for analysis of Fourier Transform Infrared (FTIR) spectra of edible oils. *Talanta*, **88**, 537–543.

9. Chou, K. T., Lee, B. I. (1993) Properties of silica gels prepared from high-acid hydrolysis of tetraethoxysilane. *Ceramics International*, **19(5)**, 315–325.

10. Twej, W. A. (2009) Temperature influence on the gelation process of tetraethylorthosilicate using sol-gel technique. *Iraqi Journal of Science*, **50(1)**, 43-49.

11. Tognovi, M. T., Rossignol, S., Bonnet, J. P. (2011) Physical-chemistry of sodium silicate gelation in an alkaline medium. *Journal of Sol-Gel Science and Technology*, **58**, 625–635.

12. Musić, S., Filipović-Vinceković, N., Sekovanić, L. (2011) Precipitation of amorphous SiO_2 particles and their properties. *Brazilian Journal of Chemical Engineering*, **28**, 89–94.

13. Arkhireeva, A., Hay, J. N. (2003) Synthesis of sub-200 nm silsesquioxane particles using a modified Stöber sol-gel route. *Journal of Materials Chemistry*, **13(12)**, 3122–3127.

14. He, S., Li, Z., Shi, X., Yang, H., Gong, L., Cheng, X. (2015) Rapid synthesis of sodium silicate based hydrophobic silica aerogel granules with large surface area. *Advanced Powder Technology*, **26(26)**, 537–541.

15. Sarawade, P. B., Kim, J. K., Hilonga, A., Quang, D. V., Kim, H. T. (2011) Effect of drying technique on the physicochemical properties of sodium

silicate-based mesoporous precipitated silica. *Applied Surface Science*, **258(2)**, 955–961.

16. Sumathi, R., Thenmozhi, R. (2015) Synthesis and characterization of spherical silica nanoparticles by Sol-Gel method. *International Conference on Systems, Science, Control, Communication, Engineering and Technology*, 204–208.

17. Zulfiqar, U., Subhani, T., Wilayat, H. S. (2016) Synthesis of silica nanoparticles from sodium silicate under alkaline conditions. *Journal of Sol-Gel Science and Technology*, **77(3)**, 753–758.

18. Darmakkolla, S. R., Tran, H., Gupta, A., Rananavare, S. B. (2016) A method to derivatize surface silanol groups to Si-alkyl groups in carbon-doped silicon oxides. *RSC advances*, **6(95)**, 93219–93230.

19. Taylor, W. R. (1990) Application of infrared spectroscopy to studies of silicate glass structure: Examples from the melilite glasses and the systems Na20-SiO2 and Na20-AI203-SiO2. In *Proceedings of the Indian Academy of Sciences*, **99(1)**, 99–117.

20. Almeida, R. M., Guiton, T. A. & Pantano, C. G. (1990) Characterization of silica gels by infrared reflection spectroscopy. *Journal of Non-Crystalline Solids*, **121(1-3)**, 193–197.

21. Perdana, I., Saribu, A. M. L. D., Bendiyasa, I. M. (2019) Solubility of sodium silicates as solid base catalyst in methanol. *AIP Conference Proceedings*, **2085 (1)**, 020053.

22. Rades, S., Hodoroaba, V. D., Salge, T., Wirth, T., Lobera, P., Labrador, R. H., Natte, K., Behnke, T., Grossa, T., Unger, W. E. S. (2014) High-resolution imaging with SEM/T-SEM, EDX and SAM as a combined methodical approach for morphological and elemental analyses of single engineered nanoparticles. *RSC Advances*, **2014(4)**, 49577.

23. Katoueizadeh, E., Rasouli, M., Zebarjad, S. M. (2020) A comprehensive study on the gelation process of silica gels from sodium silicate. *Journal of Materials Research and Technology*, **9(5)**, 10157–10165.

24. Matinfar, M., Nychka, J. A. (2024) Process mapping of the sol–gel transition in acid-initiated sodium silicate solutions. *Gels*, **10(10)**, 1–29.

25. Matinfar, M., Nychka, J. A. (2023) A review of sodium silicate solutions: Structure, gelation, and syneresis. *Advances in Colloid and Interface Science*, **322**, 103036.